



The challenges of beam polarization and keV-scale centre-of-mass energy calibration at the FCC-ee

Alain Blondel^{1,2,a} , Eliana Gianfelice³

¹ IN2P3/CNRS, LPNHE, Paris, France

² University of Geneva, Geneva, Switzerland

³ Fermilab, Batavia, IL, USA

Received: 4 May 2021 / Accepted: 22 September 2021
© The Author(s) 2021, corrected publication 2022

Abstract The capability to determine the FCC-ee centre-of-mass energies (ECM) at the ppm level using resonant depolarization of the beams is essential for the Z line shape measurements, the W mass and the possible observation of the Higgs boson s-channel production. A first analysis (Blondel A et al Polarization and centre-of-mass energy calibration at FCC-ee. [arXiv:1909.12245](https://arxiv.org/abs/1909.12245)) demonstrated the feasibility of this programme, conditional to careful preparation and a number of further developments. The existing simulation codes must be unified; the analysis and design of the instrumentation must be developed; and a detailed planning must be developed for the simultaneous and coordinated operation of the accelerator, of the continuous polarization and depolarization measurements, and of the beam monitoring devices, ensuring a precise extrapolation from beam energies to centre-of-mass energy and energy spread.

1 Introduction

A unique feature of circular lepton colliders is the precision with which the beam energies can be calibrated by means of resonant depolarization (RD). A cornerstone of the FCC-ee physics program lays in the precise (ppm) measurements of the W and Z masses and widths, as well as of lepton forward–backward asymmetries around the Z pole. The possibility of a measurement of the s-channel $e^+e^- \rightarrow H$ cross section is also under study.

In an extensive report [1], the FCC-ee Energy Calibration and Polarization working group showed that transverse polarization of the beams can be obtained around both the Z pole and up to the W pair threshold. The RD provides an instantaneous precision on beam energy that can be as good as ± 1 ppm at the Z energies, and serves as basis for a running mode where such measurements are made about 5 times an hour on pilot bunches for both electrons and positrons. The very long polarization time can be mitigated with dedicated asymmetric wigglers to be used for about 1 h at the beginning of physics fills, to polarize the pilot bunches at a level of 5–10%, before being turned off for filling the main colliding bunches. Data taking on a set of values of ECM $\simeq 2 \times E_{\text{beam}}$ associated with half-integer spin tunes $\nu_s = E_{\text{beam}}/0.4406486$ was shown to be consistent with the physics goals, without significant loss of precision.

^a e-mail: alain.blondel@cern.ch (corresponding author)

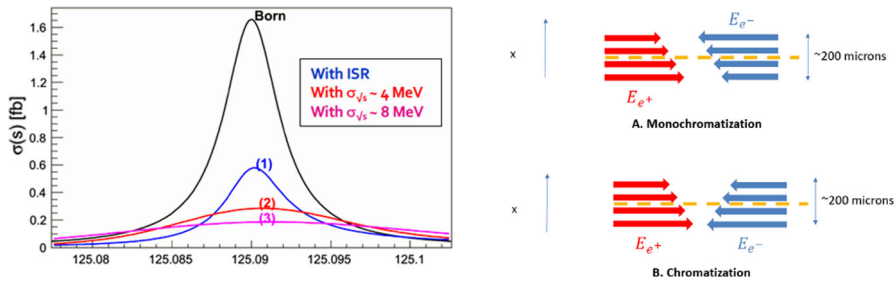


Fig. 1 Left: Higgs boson line shape. The $e^+e^- \rightarrow H$ cross section is shown as function of ECM. Black: at tree level; blue including initial state radiation; red (and magenta): adding the effect of a 4 (or 8) MeV ECM spread. Right: monochromatization. Top, the standard scheme with additional opposite sign horizontal dispersion in both beams. The average boost of the centre-of-mass varies with the x -coordinate, so the knowledge of the ECM spread requires to make the measurement of the boost distribution as function of x . Bottom: a chromatization scheme in which ECM depends on the x -coordinate

Requirements and feasible concepts for the polarization wigglers, polarimeters and the RF depolarizer were outlined. Extracting $ECM = 2\sqrt{E_b^+ E_b^-} \cos \frac{\alpha}{2}$, where α is the beam crossing angle, requires corrections for beam energy variations, RF acceleration and energy losses due to synchrotron radiation and beamstrahlung. These corrections can be made precisely enough, provided the RF accelerating system is located in a single location of the ring. Dimuon events $e^+e^- \rightarrow \mu^+\mu^-$, recorded in the detectors, provide with great precision α , the centre-of-mass energy spread, and the difference between e^+ and e^- beam energies. Beam-beam offsets bias ECM and must be corrected actively. Further monitoring to minimize both the absolute error and the relative uncertainties between the different energy settings were discussed. Elements of a program of further simulations, design, R&D and some operational requirements were outlined.

In this essay, we first complete the previous work by addressing specific issues related to a possible run on the Higgs resonance. Then, we present a list of the main remaining challenges, required studies and associated tools, R&D and tests that will need to be performed in order to make sure that this unique but challenging set of endeavours can be successfully prepared and executed.

2 A first look at beam energy monitoring issues for the Higgs resonance $e^+e^- \rightarrow H$ run

FCC-ee offers the unique opportunity to access the electron coupling to the Higgs boson [2,3]. Fig. 1 shows the cross section for the resonant production $e^+e^- \rightarrow H$ as a function of ECM. The Higgs boson is very narrow (4.2 MeV width in the SM), much smaller than the ECM spread (100 MeV) of the machine. The maximum cross section is only 1.6 pb (for a vanishing energy spread). This experiment requires to achieve simultaneously high luminosity and reduction of the ECM spread by a monochromatization scheme [4,5]; we assume this daring challenge to be realized in the following.

A successful run at the Higgs resonance requires a similar set-up as for the Z scan, with additional specifications.

- 1 The ECM setting must be exactly the Higgs boson mass within a fraction of the Higgs width, and cannot be chosen to avoid spin resonances. The 2020 value of the Higgs mass,

125.1 GeV, corresponds to a spin tune of $\nu_s = 141.95$, unfortunately close to an integer value. A solution was proposed by Oide [6]: shift the electron (resp. positron) beam energy by ± 220 MeV (resp. ∓ 220 MeV), i.e. half a unit of spin tune, thus obtaining the same ECM but (different) spin tunes, both closer to a half integer. The $e^+ - e^-$ relative energy difference is smaller than that incurred at high energies from the saw-toothing in the arcs and should be straightforward to implement.

- 2 The ECM must be known at all times to a fraction of the Higgs width. While the demand on the average value is less constraining than for the Z mass (100 keV) or the W mass (300 keV), the requirement on the stability is 20 times stronger. Fluctuations due to ground motion [1] amount to ± 90 MeV per beam at the Z resonance for the earth tides alone. Assuming the same optics are used, this would result in ECM variations of ± 250 MeV at the Higgs—or, at tidal variation maximum, up to 2 MeV/min. This can be corrected by constant adjustments of the RF frequency, using a good model of the energy variations guided by a follow-up of the beam energy with the resonant depolarizations. The development and benchmark of the energy model should take place during the Z line shape runs.
- 3 Similarly to the Z and W run, the ECM spread must be determined from experimental input. This can be done, as in [1] (section 8.1.3), using the distribution of centre-of-mass longitudinal boost determined from muon pairs; relative values of ECM can also be monitored using the invariant mass of muon pairs. The exact requirement and performance will depend on the specific monochromatization scheme (Fig. 1) and on detector performance. For the standard monochromatization scheme using opposite sign horizontal dispersion (A in Fig. 1) the average centre-of-mass boost varies across the bunch while the ECM spread is reduced; these variations and reduction must be measured by dividing the sample of muons along the horizontal axis—the vertex resolution of $\pm 3 \mu\text{m}$ is much smaller than the horizontal beam size. For a luminosity of $2 \cdot 10^{35}/\text{cm}^2/\text{s}$ and a high-mass muon pair cross section of 10pb, the ECM spread should be measurable with a relative precision of better than 10% in 20 equally populated x -bins in less than about 3 h; measuring ECM in each of so many bins with a precision of ± 2 MeV will take a few days. For the scheme where different values of ECM are spread along the x -axis (B in Fig. 1), the boost remains constant along the x -direction, while the average energy varies. In either case, the measurements of the variation of the centre-of-mass boost, ECM and ECM spread across the bunch will verify the proper realization of monochromatization; this is essential for the interpretation of the $e^+e^- \rightarrow H$ physics result.

This experiment should be scheduled after the Higgs run, since the Higgs mass must be known, and preferably be developed with the Z machine at the Z pole where statistics of muon pairs is 300 times higher. The ECM monitoring requirements are quite subtle and more stringent than for any previous measurement, and will require careful preparation. The main challenge remains to obtain high luminosity and monochromatization level simultaneously.

3 Challenges ahead

Beam polarization at FCC-ee relies on the Sokolov–Ternov effect [7]. Polarization time at the Z pole is 256 h. The time needed for the beam to reach 5% to 10% polarization, assumed sufficient for an accurate depolarization measurement, is between 14 and 29 h. By introducing for instance 8 properly designed wigglers with $B^+ \approx 0.57$ T this time is reduced by about

a factor 10. At the W pair threshold, the Sokolov–Ternov polarization time being 14 h, the time needed to reach 10% polarization is 1.6 h and wigglers are therefore not needed.

FCC-ee demanding beam parameters require an extremely well corrected machine. It has been shown [1] that large polarization is achievable at the Z pole as well as at the W-pair threshold where special corrections of spurious vertical dispersion and polarization axis may be needed, which however are not expected to deteriorate collider performance.

An important aspect to be studied is the effect of the beam–beam tune shift. Non-colliding bunches will be used for monitoring the beam energy through resonant depolarization (see Sect. 3.3). As they miss the extra focusing lens seen by the colliding bunches (beam–beam incoherent tune shift is expected to be about 0.1 per IP), their tunes will be different and they may land on a spin–orbit resonance or even on the integer resonance. We can imagine that some compromises have to be done to insure the survival of the non-colliding bunches and their polarization.

3.1 Beam polarization optimization and simulation tools

Closed orbit simulations have been performed by using MADX. The relative files have been translated into SITROS [8] language for polarization calculations. However, SITROS does not have the same MADX capabilities. Therefore, an effort for integrating polarization computations into MADX has been recently launched within the FCC-IS context. Spin tracking is also being included in BMAD toolkit [9, 10]. Integration of the spin calculation in the same set of simulations as luminosity calculations on realistic models of the machine will be essential for developing independent tuning knobs for polarization and luminosity, for optimizing the performance, and calculating possible energy versus spin tune biases.

3.2 Polarization wigglers

The choice of wiggler location, parameters and number results from the need of decreasing polarization time keeping the beam horizontal emittance, energy spread and additional energy loss within limits. Although it will be impossible to operate them with a full machine because of the excessive synchrotron radiation, a detailed design of the wigglers, especially concerning the management of the 900 KeV critical energy photons, is needed. However, we do not expect this to be a critical issue.

3.3 Polarization operation

Without wigglers bunches need 29 h at the Z pole energy to reach 10% polarization. Colliding bunches lifetime being about 1 h (Bhabha scattering limited), non-colliding bunches will be used for energy calibration. Polarization operation could look as follows. Some hundreds non-colliding bunches with a somewhat reduced population ($N_b \approx 1e10$), their lifetime being limited by Touschek effect, will be first injected with wigglers switched on until polarization reaches between 5% and 10% when wigglers will be switched off and the remaining bunches injected. Monitoring the energy by targeting one different bunch each 10 min, there are about 17 h during which the newly injected non-colliding bunches can reach the needed polarization without wigglers. Operation is much relaxed at the W-pair threshold where wigglers are not needed and the Touschek effect less severe.

3.4 Sources of ECM biases

Depolarization occurs when spin precession and depolarizing field frequency are in resonance. Due to the high precision required in the determination of the CM energy, a number of factors must be considered, keeping in mind that the energy measured by resonant depolarization is the *average* beam energy over the accelerator. A first analysis of various sources of systematic errors is found in [1].

Effects related to possible beam energy drifts during the physics run (main dipole field, horizontal orbit and corrector settings, machine circumference, RF phasing), call for a frequent energy monitoring (\approx each 10 min) and the development of models for interpolation as done at LEP.

The relationship $\nu_{spin}=a\gamma$ between spin tune and relativistic γ factor holds only for a perfectly planar ring without solenoids. For FCC-ee the effect of the experiment solenoids is negligible.

Momentum compaction dependence on energy, non-vanishing vertical closed orbit and electric fields non-perfectly aligned to the beam orbit also break the relationship. The impact of orbit effects can be evaluated through simulations and preliminary studies indicate that they are sufficiently small for the well corrected orbit required by luminosity operation. The impact of the momentum compaction chromaticity depends upon energy spread and it results particularly large for colliding bunches which at 45 GeV have a factor three times larger energy spread due to beamstrahlung. From the machine model, the relative systematic error introduced by this effect is about $2.5e-6$ for both Z pole and W pair threshold.

The beam energy is azimuth-dependent due to synchrotron radiation, RF stations and wake fields. The average beam energy will be therefore different from the beam energy at the IP. The correction of these effects requires a good knowledge of the guiding field ($10e-4$ is sufficient and achievable) and an evaluation of the additional synchrotron radiation due to the finite closed orbit.

The energy loss related to the dominant resistive part of the longitudinal impedance can be measured resorting to the orbit dependence upon bunch intensity at $D_x \neq 0$ locations. The achievable accuracy for FCC-ee must be evaluated.

Other effects which introduce systematic errors such as energy-dependent particle densities at the IP, counter-rotating bunch fields and longitudinal space charge have negligible effects.

3.5 Control of opposite-sign dispersion and collision offsets

This effect has been extensively documented in [1]. An offset between colliding beams affects the CM energy if the dispersion of the two rings has opposite sign. For parasitic effects, the CM energy error is

$$\Delta\sqrt{s} = -\frac{\Delta z^* \sigma_E^2}{2\sigma_z^2 E_0} \Delta D_z^* \quad z = x, y$$

ΔD_z^* and Δz^* being the difference of the dispersion of the two rings at the IP and the beam offset, respectively. The effect is particularly severe in the vertical plane. Based on simulations it is $\sigma_{D_y} \approx 10 \mu\text{m}$. At the Z pole, it is

$$|\Delta\sqrt{s}| = 0.048 \times |\Delta y^* \Delta D_y^*| \text{ [keV]}/[\text{nm}]^2$$

Assuming $\Delta D_y^*=10 \mu\text{m}$, to keep the error below 100 keV the average vertical offset between the two beams must be known to $\leq 0.2\text{nm}$, i.e. about 0.6% of the vertical beam size.

Due to the required accuracy, this is one of the most challenging aspect of the ECM determination at FCC-ee. A way forward is to investigate diagnostics allowing control of the beam–beam offsets and the measurement of residual dispersion and the interaction point. This will allow ECM shifts to be reduced and monitored, but should also benefit the optimization of luminosity. The following methods for the IP collision monitoring have been suggested.

- 1 Luminosity scans in the vertical direction, possibly using fast luminosity monitors, can be used to maximize the luminosity. The precision will depend upon the possibility to explore large excursions. The required frequency of this somewhat intrusive technique will in turn depend on the achievable precision.
- 2 Colliding-beam offsets result in measurable beam–beam deflection at the beam collision frequency, which can be picked up with the beam position monitors.
- 3 Another possibility is to measure high-energy photons from radiative Bhabha scattering or beamstrahlung at the collision point: calorimeters could be situated in the first bending magnets downstream of the IP; movements of the spot of zero angle high energy photons emitted in the collisions constitute a sensitive indicator of collision offset, and might be more practical than luminosity scans.
- 4 Shifts in the position of the high-energy photon spot, or in the amplitude of the beam–beam deflection, would indicate residual vertical dispersion each time the RF frequency was modified to follow the ground motion.
- 5 It was signalled in [1] that the effect in the horizontal dimension is difficult to scan. The methods designed in Sect. 2 to monitor the monochromatization, together with the detection in the experiments of movements of the collision point upon changes in the RF frequency, might be operational for such monitoring and should be further studied.
- 6 The actual crossing angle can be very precisely measured in the experiments [1] both in x and y , and may shed light on this question.

The points 2, 3, 4, 5 and 6 above are intrinsically passive methods which should be further investigated. The whole set of diagnostics and procedures should be devised and integrated in the control system with the aim of becoming as automatic as possible and carefully recorded.

3.6 Depolarization, kicker and operation mode

For a perfectly flat storage ring, the resonant depolarization frequency corresponds to the average of the beam energy over the ring and over the electron population of the bunches. The measurement is described in [11]. One of the issues that was raised in the study is the fact that the resonant frequency corresponding to beam energy is not the only possible one, its synchrotron side bands can also cause depolarization, leading to a possible mistake in the true measurement by, e.g. one or several synchrotron tune. The effect is particularly visible at the WW threshold energy (80 GeV per beam) where the larger energy spread excites the synchrotron resonances. Simulations showed that the way the excitation frequency is swept has an impact on the result and that, while the resonance is strong and unambiguous at the Z energy, it appears weak at the W threshold energy and best is to sweep the frequency in small steps, interleaved with precise polarization measurements as was done for the LEP measurements (Fig. 2). Given that the depolarization signal at W energies is a weak relative depolarization of 4%, it is clear that further optimization of the process will be necessary. It is also hoped that the precision can be improved to better than the statistical precision of $\mathcal{O}(200 \text{ keV})$ on the W mass measurement. In particular, it should be verified that the depolarizer that was proposed (the LHC transverse kicker) is of sufficient strength.

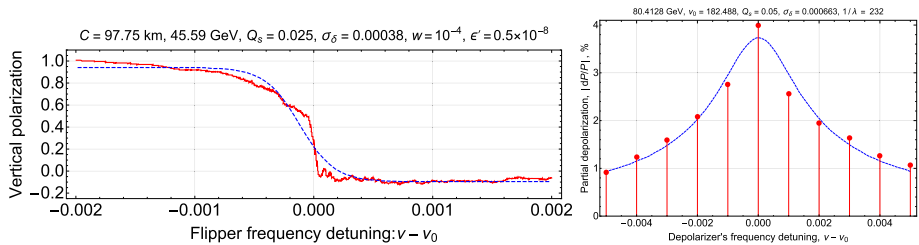


Fig. 2 Simulation of a frequency sweep with the depolarizer on the Z-pole showing a very sharp depolarization at the exact spin tune value. At the WW threshold, the energy spread is too large to perform a wide frequency sweep, progressing in little steps is required

In conclusion, the resonant depolarization process and its sensitivity to the energy spread and synchrotron tune should be further studied to optimize the procedures and the machine settings. The precision obtainable at the W threshold energy should be clarified and, if possible, improved.

3.7 Polarimeter implementation and spectrometer operation

The proposed polarimeters [12] are based on the detection of both photons and e^\pm emitted in Compton scattering of a polarized laser with the e^\pm beam. The main conceptual parameters and a possible placement in the rings have been described in [1]. The measurement of the polarization need not be very precise in absolute scale, but it must be fast and sensitive. Its main function is to measure the polarization and depolarization of the pilot bunches. However, it will be important for two other functions.

1. The polarimeter should be able to detect any residual polarization both transverse and longitudinal, of the colliding bunches, down to a level that cannot affect the physics cross sections and asymmetries in the physics experiments. This point has not been investigated so far and should be quantified.
2. The polarimeter also analyses the momentum of the final state e^\pm . This measurement can play an important role to track the beam energy variations and monitor the relative point-to-point energy uncertainties, independently of the possible systematic errors in the relation between beam energy and spin tune.

In addition it offers several by-products. The measurement of the photon beam size and its movements with RF frequency changes will provide amplified of the circulating beam size and residual angular dispersion. The difference in scattered photons between the pilot bunches and colliding bunches will provide sensitive measurements of the beam–beam effects, etc.

On a more practical side, the polarimeter construction presents much work to do and several challenges which are listed in the following.

- Define electron bunch populations, beam sizes, specify desirable laser spot size and intensity.
- Specify parameters of the laser (wavelength, repetition rate, intensity, instantaneous and average power, required precision of laser polarization)
- Specify sizes and rates for the detectors of scattered photons and electrons
- The insertion in the storage ring might be the most delicate of all tasks. After a study of the possible location given the anticipated synchrotron radiation exposure, the design of laser ports and mirrors, and of the final state exit ports, in a storage ring where a current

Table 1 Calculated uncertainties on the quantities most affected by the centre-of-mass energy uncertainties, under the final systematic assumptions

Observable	Statistics	$\Delta\sqrt{s}_{\text{abs}}$ 100 keV	$\Delta\sqrt{s}_{\text{syst-tp}}$ 40 keV	Calib. stats. 200 keV/ $\sqrt{N^i}$	$\sigma\sqrt{s}$ 85±0.05 MeV
m_Z (keV)	4	100	28	1	–
Γ_Z (keV)	4	2.5	22	1	10
$\sin^2 \theta_W^{\text{eff}} \times 10^6$ from $A_{\text{FB}}^{\mu\mu}$	2	–	2.4	0.1	–
$\frac{\Delta\alpha_{\text{QED}}(m_Z^2)}{\alpha_{\text{QED}}(m_Z^2)} \times 10^5$	3	0.1	0.9	–	0.1

Bold values indicate the dominant sources of uncertainties

of 1.3 A will be circulating will be critical. The transverse mode coupling to circulating beams must be considered.

- The laser light box is the beating heart of the system. The desired polarization states must first be established, controls and monitoring in synchronization with accelerator bunches must be foreseen and automatized.
- The photon counter must be designed in anticipation of the spot size at all energies, and be able to deal with both pilot bunches and colliding ones. A movable SR shielding must be foreseen.
- The spectrometer and electron asymmetry monitor will require a dedicated design of the magnet and of the mechanical alignment, possibly monitoring, of distance between the scattered e^\pm detector and the photon detector.
- The overall data acquisition, the operator interface for input and output of results will require a good understanding of the operations to be foreseen. A connection with other polarization-related operation systems (spin correctors, injection, etc.) must be foreseen.

The system of polarimeters is considerably more complex than the LEP polarimeter, and constitutes a small particle physics experiment in its own right. It could be the object of a very stimulating worldwide collaboration.

3.8 Point-to-point ECM systematics

We reproduce in (Table 1) the final error table of Ref. [1]. It shows very clearly that the most meaningful electroweak observables, the Z width and the lepton asymmetries, have uncertainties governed by point-to-point systematic errors in the centre-of-mass energy calibration.

Two possible levers against these have been listed in [1]. The polarimeter in its spectrometer function, already described in Sect. 3.7 and the direct measurement of the centre-of-mass energy using the invariant mass distribution of muon pairs. The latter will be affected by QED effects, which have a non-trivial energy dependence around the Z peak, and constitutes a considerable challenge for theoretical calculations. Another challenge will be the stability of the momentum measurement, for which it seems that the most stable fixed candle could be the measurement of the $J/\psi \rightarrow \mu\mu$ invariant mass in the large samples of hadronic Z decays across the Z resonance; this work has started [13].

4 Conclusions and acknowledgements

The high precision centre-of-mass energy calibration at FCC-ee offers unique opportunities. A number of important challenges have been outlined in view of a technical feasibility study. Among the most striking ones are: the feasibility of polarization and depolarization in a machine dedicated to high luminosity; the integration of the proposed polarimeter/spectrometer in an Ampere-class machine; the control of collision conditions to reduce systematic errors; the minimization of point-to-point systematic uncertainties.

It is a pleasure to thank all the authors of [1] for enjoyable collaboration and illuminating discussions. We look forward to tackle the considerable challenges of historically precise measurements as a great teamwork between the accelerator and experiment communities.

Funding This project is co-funded from the European Union's Horizon 2020 research and innovation programme under grant agreement No 95175.

Open Access This article is licensed under a Creative Commons Attribution 4.0 International License, which permits use, sharing, adaptation, distribution and reproduction in any medium or format, as long as you give appropriate credit to the original author(s) and the source, provide a link to the Creative Commons licence, and indicate if changes were made. The images or other third party material in this article are included in the article's Creative Commons licence, unless indicated otherwise in a credit line to the material. If material is not included in the article's Creative Commons licence and your intended use is not permitted by statutory regulation or exceeds the permitted use, you will need to obtain permission directly from the copyright holder. To view a copy of this licence, visit <http://creativecommons.org/licenses/by/4.0/>.

References

1. A. Blondel et al., Polarization and centre-of-mass energy calibration at FCC-ee. [arXiv:1909.12245](https://arxiv.org/abs/1909.12245)
2. D. d'Enterria, Higgs physics at the future circular collider, *PoSICHEP2016* (2017) 434. [[arXiv:1701.02663](https://arxiv.org/abs/1701.02663)]
3. D. d'Enterria, A special Higgs challenge (1): measuring the electron Yukawa coupling via s-channel Higgs production. A future Higgs and Electroweak factory (FCC): challenges towards discovery, EPJ+ special issue, Focus on FCC-ee
4. F.C.C. Collaboration, A. Abada et al., FCC-ee: The Lepton Collider. *The Eur. Phys. J. Special Top.* **228**, 261–623 (2019)
5. ATLAS collaboration, G. Aad et al., Search for the Higgs boson decays $H \rightarrow ee$ and $H \rightarrow e\mu$ in pp collisions at $\sqrt{s} = 13$ TeV with the ATLAS detector. [arXiv:1909.10235](https://arxiv.org/abs/1909.10235)
6. K. Oide, Private communication, FCC week, Amsterdam 2018
7. A. A. Sokolov, I. M. Ternov, On Polarization and spin effects in the theory of synchrotron radiation. *Sov. Phys. Dokl.* **8** (1964) 1203–1205. http://inspirehep.net/record/918891/files/HEACC63_II_576-581.pdf (1964)
8. J. Kewisch, Computation of electron spin polarization in storage rings, in *Proceedings of Europhysics Conference on Computing in Accelerator Design and Operation*, Berlin, Germany, September 20–23 (1983). https://link.springer.com/content/pdf/10.1007/3540139095_115.pdf
9. D. Sagan, Bmad manual: software toolkit for charged-particle and X-ray simulations. <https://www.classe.cornell.edu/bmad/manual.html>
10. D. Sagan, Bmad: a relativistic charged particle simulation library. *Nucl. Instrum. Meth. A* **558**, 356–359 (2006)
11. N. Alipour Tehrani et al., FCC-ee: Your Questions Answered, Sections 8.2 and 23.6, in *CERN Council Open Symposium on the Update of European Strategy for Particle Physics (EPPSU)* Granada, Spain, May 13–16, 2019, ed. by A. Blondel and P. Janot (2019). [arXiv:1906.02693](https://arxiv.org/abs/1906.02693)
12. N. Muchnoi, FCC-ee polarimeter. [arXiv:1803.09595](https://arxiv.org/abs/1803.09595)
13. E. Leogrande, Point-to-point uncertainty on sqrt(s) with dimuons and momentum scale stability, FCC-ee Physics Performance meeting. <https://indico.cern.ch/event/982690/>. 14 Dec 2020